Egypt. J. Chem. **Vol. 67**, No. 9 pp. 507 - 521 (2024)

Egyptian Journal of Chemistry

http://ejchem.journals.ekb.eg/

A Highly Selective Potentiometric Sensor for Detection of Zn(II) in Petroleum Water Samples Using Carbon Paste Electrode Based on Molecular Imprinted Polymer

Yassmin Emad[a], Tamer Awad Ali[b*], Gehad G. Mohamed[c,d], Madiha Hassan[a], Abdel El-Fatah Bastawy[a]

[a] *Chemistry Department, Faculty of Science, Helwan University, 13518 Helwan, Egypt*
[b] *Egyptian Petroleum Research Institute (EPRI), 11727 Cairo, Egypt*
[c] *Chemistry Department, Faculty of Science, Cairo University, 12613 Giza, Egypt*
[d] *Nanoscience Department, Basic and Applied Sciences Institute, Egypt-Japan University of Science and Technology, Ne Borg El Arab, Alexandria, 21934, Egypt*

Abstract

For the purpose of determining the presence of zinc(II) in petroleum water samples, a molecular imprinted polymer (MIP) based modified carbon paste potentiometric method was described. Methacrylic acid monomers and ethylene glycol dimethacrylate were used in the polymerization process to create the MIP. The generated imprinted polymer was evaluated using flame atomic absorption spectrometry, Fourier transform infrared spectroscopy (FT-IR), and proton nuclear magnetic resonance (^{1}H-NMR). It was then used as a sorbent for selective magnetic solid phase extraction of zinc(II) ion. Using MIP as a suitable neutral carrier, a label modified carbon paste electrode (MCPEs) that is highly selective to Zn(II) ions was created. For MCPEs (Sensors I and II), they demonstrated a linear concentration range from $1.0x10^{-7}$ to $1.0x10^{-1}$ mol L^{-1} with Nernstian slopes of 28.43±0.63 and 29.27±0.48 mV $decade^{-1}$, respectively. The sensors (I) and (II) had lifetime of 97 and 115 days and response time of 7 and 5 s, respectively. The suggested electrodes were successfully applied in determining the Zn(II) ion concentrations in petroleum water samples. The outcomes were comparable to those from atomic absorption spectroscopy (AAS) in actual spiked petroleum water samples.

Keywords: Chemically modified carbon paste sensor; Zn(II) determination; Imprinted molecular polymer; Potentiometric sensor; Petroleum water sample

1. Introduction

A 3D-polymeric network may be made particularly and selectively by molecular imprinting, which also provides contact sites and a coordination sphere surrounding the template molecule. These holes complement the size and form of a target species. Due to its selective identification, high capacity for adsorption and great selectivity via the memory effect of template ions, which is influenced by variables including the affinity of template ions and ligands, coordination number, charge, and size of metal ions influences [2], ion imprinting technology (IIT) has lately emerged as a very useful and common technique. Zinc has a lengthy history of use despite being very uncommon in nature. Its compounds are widely employed in a variety of industries, including electroplating, medicines, rubber, wood preservatives, paint, ointments, dye and batteries. It may be found in these sectors' wastes and effluents as ZnCl2, ZnSO4, ZnO, and ZnS. For people, animals, and plants, zinc is a necessary trace element [3]. It is essential for several biological processes and is involved in over 300 enzymes in the human body. It is crucial to evaluate the amount of zinc present in these wastes since a high dosage of zinc (10–15 times the RDA, or 10-15 mg/day; RDA stands for recommended dietary allowance) can lead to nausea, vomiting, severe anemia, pulmonary manifestations, and renal failure [4]. A health issue that is at least as significant as zinc overconsumption is zinc consumption too low. Lack

*Corresponding author e-mail: dr_tamerawad@yahoo.com.; (Tamer Awad Ali).
Received date 13 November 2023; revised date 25 January 2024; accepted date 12 February 2024
DOI: 10.21608/EJCHEM.2024.247470.8869
©2024 National Information and Documentation Center (NIDOC)

of zinc in the diet can lead to impaired immunological function, appetite loss, sluggish wound healing, and poorly formed male sex organs [5]. The measurement of zinc therefore has significance considering its toxicity and lack [6]. Heavy metal ions may be revealed at low concentrations using a variety of techniques, such as spectroscopic ones like inductively coupled plasma-optical mass spectrometry and atomic absorption spectrometry, as well as electrochemical ones like potentiometry employing ISEs [7-9]. The spectroscopic approaches need highly skilled personnel, high instrument and operating expenses, preparatory sample preparation that raises the possibility of sample contamination, and challenging instrument setup. Using these approaches for in-field, real-time measurements is challenging due to all of these factors [10].

Since ion selective electrodes provide precise, quick, non-destructive, and affordable techniques of examination, they continue to be a fascinating field of analytical study [11]. Also, these devices allow for online monitoring, although efforts to create effective zinc-selective electrodes have not been very successful up to this point. The majority of them have a long reaction time, limited lifespan, and poor selectivity, sensitivity, and stability. Poly (vinyl chloride) (PVC) membrane electrodes for s- and p-block metal ions have been constructed using a substantial variety of macrocycles, ranging from crown ethers to calixarene derivatives [12, 13]. The formation constant of s- and p-block metal complexes is widely known to be dramatically reduced when certain oxygen atoms in crown ethers are replaced by nitrogen atoms, while the stability of the complexes formed with soft transition and heavy metal ions is noticeably increased. A Zn(II) selective electrode was made using dithiazone (I), an electroactive substance with NNOO atoms serving as ligating sites, which was successfully synthesized and employed in the PVC matrix. The results are described in this study. Environmental, pharmacological, and biological sample detection using electrochemical methods, an attention has been drawn to molecularly imprinted polymer (MIP)-based sensors. [14–18]. Due to their simplicity of creation, cheap cost, and high renewability, molecular imprinting is a strong approach that involves creating a polymer matrix with an affinity for a specified "template" molecule or ion through the polymerization process [19-22]. Moreover, these sensors' sensitivity and selectivity may be increased using a variety of modification strategies [26, 27]. Molecular imprinting polymer (MIP) ionophore-based electrochemical sensors are used to recognize the target analyte selectively and precisely [28]. The primary component of the polymeric membrane, the integrated ionophore interacts with the analyte to determine membrane selectivity (cavity size geometry of the molecules and kind of functional group that leads to particular contact) [29, 30]. The MIP is typically created by polymerizing monomers with an initiator, cross-linker, and templet (the target molecule) [31]. During the polymerization process, the inherent molecular group of monomers and the target molecules mostly created hydrogen bonds or electrostatic interactions. After that, the targeted template molecules are recognized using imprinted cavities left behind by the removal of the target molecules to create holes on the polymeric matrices' surface [32, 33].

Potentiometric measurements have recently been used to achieve a notable feat in MIP-based electrochemical sensing. Several potentiometric sensors were developed based on MIP and incorporated in polyvinyl chloride membranes when various plasticizers were present. These polymeric layered membranes were then applied to the surfaces of various electrodes (ex: platinum electrode, graphite electrode, GCE, and gold electrode). For all of these potentiometric sensors, great stability, outstanding repeatability, and high reusability were observed. One of the greatest options for improving the electrochemical electrodes sensitivity is graphite electrode, which also increases mechanical strength, molecular barrier, and electrical conductivity capabilities. Also, a review of the literature revealed that none of the electrochemical approaches had been used to the identification of Zn(II) ions. Recently, a significant development in MIP-based electrochemical sensing has been made using So, the primary objective of the current work is to provide straightforward potentiometric techniques for identifying and tracking the Zn(II) ion in water samples. These sensors were created with the MIP methodology. Methacrylic acid (MAA), ammonium persulfate, and zinc served as the template for the MIP's synthesis. 2,2'-azobisisobutyronitrile (AIBN) served as the initiator while ethylene glycol dimethacrylate (EGDMA) served as the cross-linker.

The electrodes responded well, and the outcomes were favorable. With excellent accuracy, low standard deviation, and relative standard deviation values, they were able to effectively employ for the detection of Zn(II) ions in petroleum water samples. They can be employed as portable electrodes in field measurements for the routine analysis of Zn(II) ions, per the statistical analyses.

2. Experimental

2.1. Chemicals and Reagents

All chemicals and reagents used in the fulfillments were of analytical reagent grade. Their names and sources were given in the Supplementary materials.

2.2. Synthesis of MIP

The molecularly imprinted polymer (MIP) for Zn(II) ion was synthesized by the thermal polymerization technique and the procedure was given in detail in the experimental part.

2.3. Water Samples

The source of water samples included in this study was given in the Supplementary materials.

2.4. Zn(II) ion Solutions

A detailed description is given in the Supplementary materials.

2.5. Apparatus

All the apparatus used in the measurements were given in the Supplementary materials

2.6. Procedures

2.6.1. Preparation of Zn(II) imprinted polymer

Thermal polymerization procedure was followed and was described as given in the Supplementary materials.

2.6.2. Preparation of a carbon paste electrode modified chemically

The carbon paste electrodes modified were fabricated as given in details in the Supplementary materials.

2.6.3. Potentiometric titration of Zn(II) in pure solutions

The various manufactured sensors were used to potentiometrically monitor the titration process as given in the Supplementary materials [34].

2.6.4. Potentiometric calibration of Zn(II) in pure solutions

The new modified CPEs were calibrated as illustrated in the Supplementary materials. The calibration curves were constructed as shown in Figure 1 [35, 36].

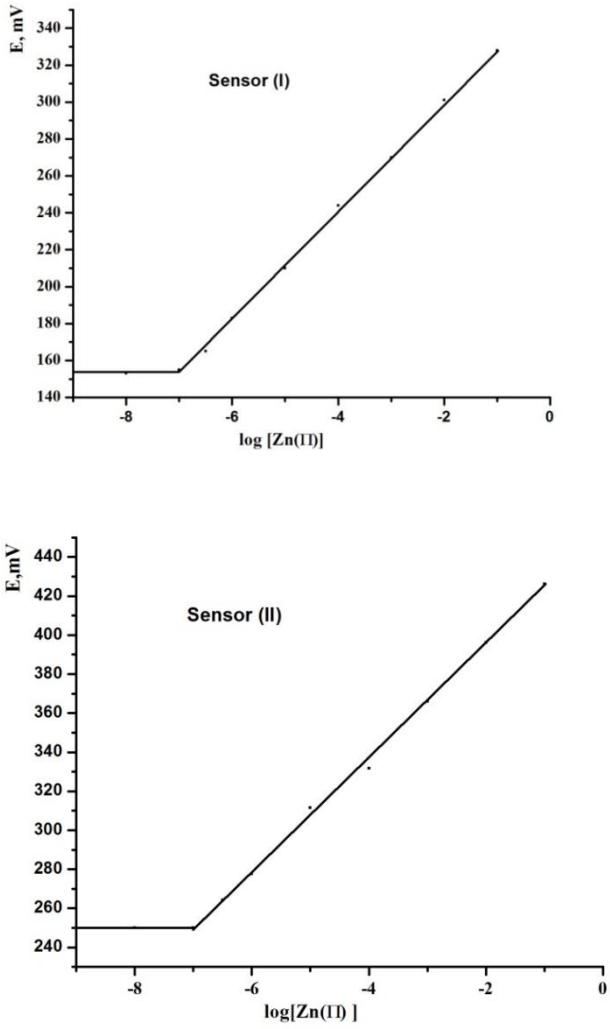

Figure 1: Effect of calibration on the performance characteristics of MCPEs of Sensor (I) and Sensor (II)

2.6.5. Determination of Zn(II) in real spiked water samples

Zn(II) concentration was estimated via NaTPB potentiometric titration solution using modified CPEs as working electrodes and the method was given in detail in the Supplementary materials.

3. Results and Discussion

3.1. Characterization of the MIP

It is noteworthy that this ratio was used in the current study to synthesize the zinc(II) molecularly imprinted polymer because a template: functional monomer: cross-linker molar ratio of about 1: 4: 20 has provided highly suitable performance characteristics in the creation of several non-covalent MIPs [37, 38]. Methacrylic acid (MAA) is the functional monomer that is used the most frequently used. The carboxyl group on this monomer is a superior hydrogen bond giver and acceptor in addition to the strong ionic connections that MAA may create with the basic functional groups on the template [37, 38]. Care must be taken while selecting the cross-linking monomer because it has a major impact on the MIP's structure and chemical environment. Two acrylate groups on the most common cross-linker, EGDMA, allow it to create more stiff polymers. The MIPs generated by this increased stiffness have been demonstrated to have better capacities and selectivity [37, 38]. The MIP particles and control polymer created using the non-covalent imprinting technique were characterized using FT-IR and ^{1}H-NMR.

3.1.1. The FT-IR spectral study

The structure of synthetic polymers, such as un-leached MIP and leached MIP, is clarified using IR spectra. The polymers' IR spectra are comparable, indicating that their backbone structures are identical [37]. The absorptions resulting from the stretching of the carboxyl OH group (3500 cm^{-1}), the carbonyl group (1730 cm^{-1}), the C-O group (1260 cm^{-1}) and the C-H vibrations (756, 1390, 1460, and 2956 cm^{-1}) were seen in the IR spectra. This characteristic is evident from the fact that the absorbances at 2956, 1730, 1260 and 1460 cm-1 were attributable to the C-H stretch of the methylene group, the carbonyl group, the C-O and the C-H bend of -CH_2 stretching vibrations for the MIP which are relatively stronger than for non-imprinted polymer [37]. This contrast showed that the inclusion of ethylene glycol dimethacrylate during the manufacture of the polymer is enhanced when the imprint molecule (zinc) is present [37]. The bands at 1476 and 1422 cm^{-1} are what cause aromatic ring's C=C vibrations.. The existence of symmetric and antisymmetric C-O-C bond vibrations were evidenced from the existence of the bands at 1315 and 1089 cm^{-1}, respectively. The existence of the COOH group is shown by the band at 1735 cm^{-1}, and that of the O-H deformation and C-O stretching is indicated by the band at 1231 cm^{-1}. New bands at 524 and 470 cm^{-1} were found in the spectra of un-leached MIP by contrasting its spectrum with that of leached MIP. These bands were given to the Zn-O and Zn-S stretching vibrations of the Zn-polymer template. As illustrated in Figure (2), the existence of these bands demonstrated that template molecules were successfully anchored to the polymer throughout the polymerization process [39-41].

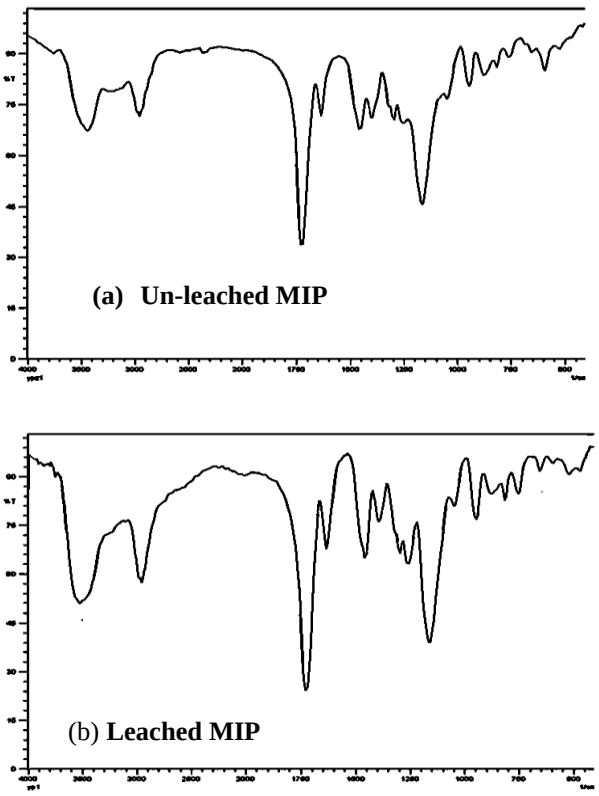

Figure 2: FT-IR spectra of the synthesized polymer for un-leached (a) and leached (b) MIP.

3.1.2. The ^{1}H-NMR spectral study

^{1}H-NMR spectrum for leaching MIP Figure [3] showed different peaks at δ (ppm) = 1.02-1.15 (m, 12H, CH_2), 1.86 (t, 2H, S-CH_2-CH_2), 2.49 (t, 2H, O-CH_2-CH_2), 3.34 (t, 2H, S-CH_2-CH_2), 3.53 (s, 3H, S-CH_3), 3.59 (t, 2H, O-CH_2-CH_2), 4.34 (d, 4H, ArH), 5.68 (d, 4H, ArH) and 6.01 ppm (s, 1H, CH-N). Furthermore, ^{1}H-NMR spectrum for unleaching MIP as shown in (Figure 3) revealed different peaks at δ (ppm) = 1.08-1.14 (m, 12H, CH_2), 2.72 (t, 2H, S-CH_2-CH_2), 3.59 (t, 2H, O-CH_2-CH_2), 4.09 (t, 2H, S-CH_2-CH_2), 4.11 (s, 3H, S-CH_3), 4.79 (t, 2H, O-CH_2-CH_2), 5.59 (d, 4H, ArH), 6.92 (d, 4H, ArH) and 7.77 (s, 1H,

CH-N) [42]. It is clear that the shift in band position can be accounted for the change in carbon skeleton as the results of Zn-dithiazone complex incorporation in the polymer structure.

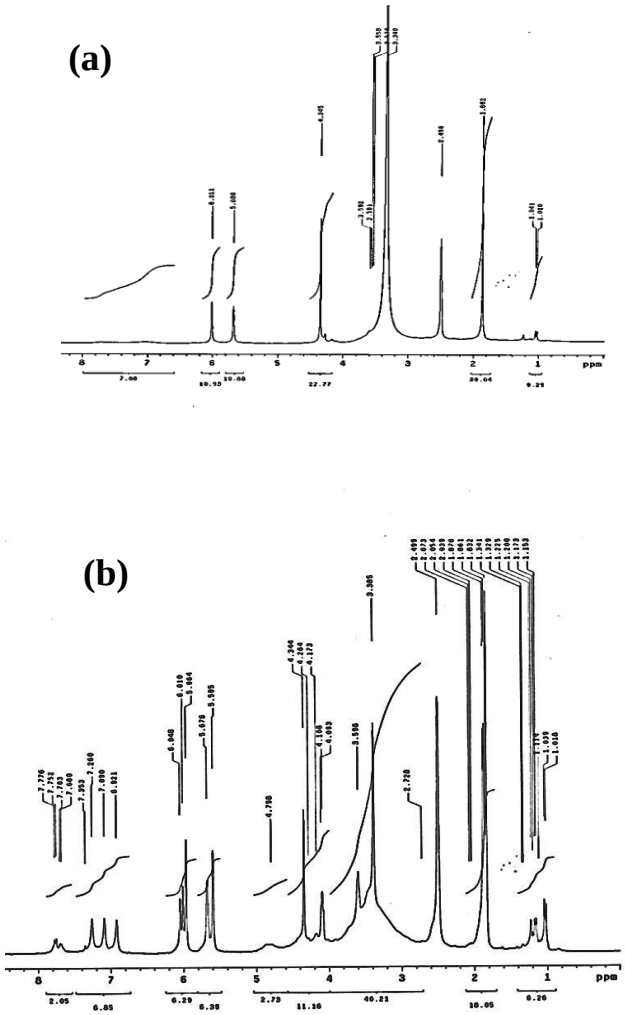

Figure 3: ^{1}H-NMR spectra of the synthesized polymer for un-leached (a) and leached (b) MIP.

3.2. Effect of ionophore content

The electrode potential is determined by chemical equilibrium at the membrane or electrode/solution interface when there is enough electroactive material in the matrix to accomplish acceptable ionic exchange (selective extraction of the target ion). If they are present in excess, the membrane network becomes oversaturated, which impedes the ionic exchange process and results in subpar performance. Zn(II) imprinted polymer weights were varied as 5, 7.5, 10, 12.5, 15, and 17.5 mg (weight/weight%). After performing a potentiometric titration on each electrode, it was found that the MCPEs sensors' respective potential breaks at the end point were 117, 135, 190, 255, 230, and 209 mV mL^{-1}. These electrodes provided consistent and acute inflections at the termination point (255 mV mL^{-1} for MCPE). These findings suggested that the 12.5 mg Zn(II) imprinted polymer ionophore for the MCPE sensor was used to assess the largest potential break at the end point. The overall potential change, however, reduced as the amount of Zn(II) imprinted polymeric ionophore increased beyond 12.5 mg, as seen in Figure 4. It should be emphasized that the inclusion of a lipophilic anion improved the selectivity, response behavior, and ohmic resistance of cation-selective electrodes while simultaneously raising their sensitivity in situations when extraction is subpar.

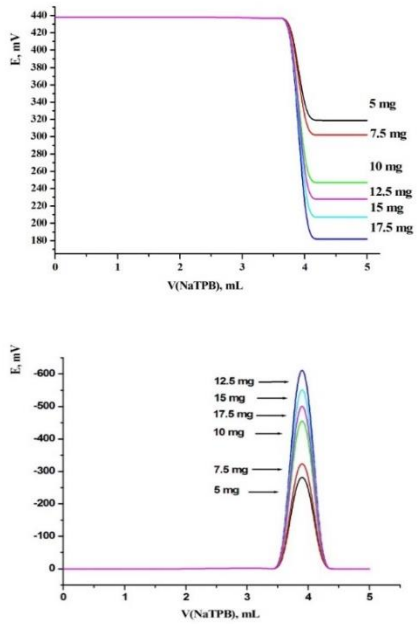

Figure 4: Effect of ionophore contents on the performance characteristics of MCPEs sensors.

3.3. Effect of plasticizer

Using five different solvents with varying polarity, including o-NPOE, TCP, DOP, DBP, and DOS, it was determined how the kind and concentration of the solvent mediator (plasticizer) affected the features of the Zn(II) modified carbon paste sensors. Plasticizers not only make the sensor easier to use, but they also significantly lengthen the

electrode's life and increase its stability and operating concentration range. The potential break at the electrodes' end points (MCPEs) was measured and determined to be, respectively, 268, 255, 225, 190 and 135mV mL^{-1} The outcomes demonstrated that, as shown in Figure 5, the electrodes made employing the plasticizers with the highest dielectric constants (o-NPOE and TCP) had the best performance.

3.4. Effect of soaking time

It is necessary to soak freshly made electrodes in order to activate the carbon paste layer's surface and create an incredibly thin gel layer where ion exchange takes place. A fast establishment of equilibrium is unquestionably a requirement for a fast potential response, so the performance characteristics of the zinc ion-selective electrodes were investigated as a function of soaking time. This preconditioning process necessitates various times depending on diffusion and equilibration at the electrode-test solution interface. To do this, CPE sensors were immersed in a 1×10^{-2} mol L^{-1} Zn(II) solution, and titration curves were drawn, from which the total potential changes and the potential break at the end point were recorded after 0, 5, 10, 15 and 60 min. The maximum total potential change and the potential break at the end point were obtained at 25 °C, and 5 min was found to be the ideal soaking period. It was discovered that as the soaking time increased, the overall potential change shrank. While not in use, the electrodes should be kept in a refrigerator. Figure 6 depicts the Zn(II) end point, potential break at the end point, and overall potential changes using modified carbon paste potentiometric sensors.

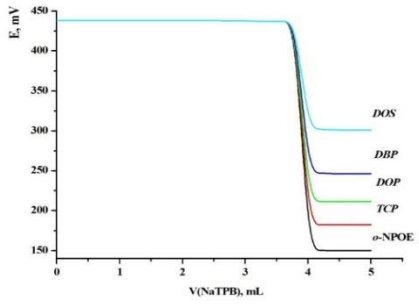

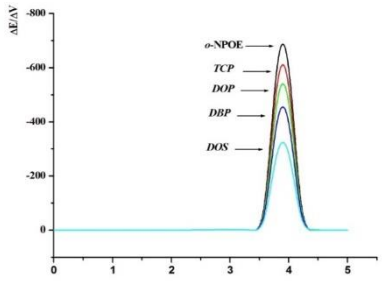

Figure 5: Effect of plasticizer type on the performance characteristics of MCPEs sensor.

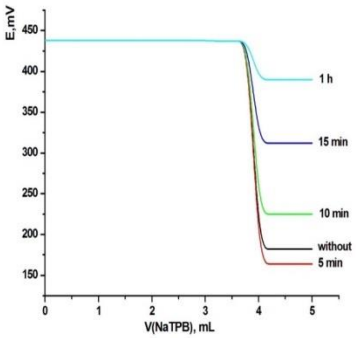

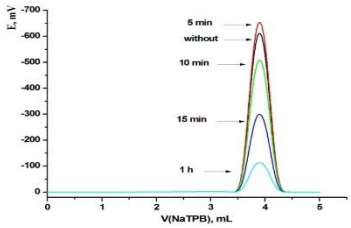

Figure 6: Effect of soaking time on the performance characteristics of MCPEs sensors.

3.5. Response time and Reversibility of the Electrode Response

One of the key features of any synthetic sensor is response time. Response time for potentiometric sensors is defined as the typical time needed to realize a voltage that is 0.1 mV or less from the most recent steady state potential. Using CPEs (Sensors I and II) with improved synthesis, the anode potential in Zn(II) arrangements ($1.0x10^{-7}$-$1.0x10^{-1}$ mol L^{-1}) was calculated (Figure 7). The recommended sensors' MCPE (sensors I and II) respond in just 7 and 5 s, respectively. The short reaction times can be explained by the presence of carbon particles inside of these electrodes, which operate as a conductor and are ringed by a very thin coating of TCP. A similar

approach was used in the other way to assess the electrode's reversibility. High sample concentrations were measured first, followed by low sample values. It demonstrates that, despite equilibrium values being longer to attain than low-to-high sample concentrations, the potentiometric responses of the sensors were reversible and had no memory effect (Figure 7).

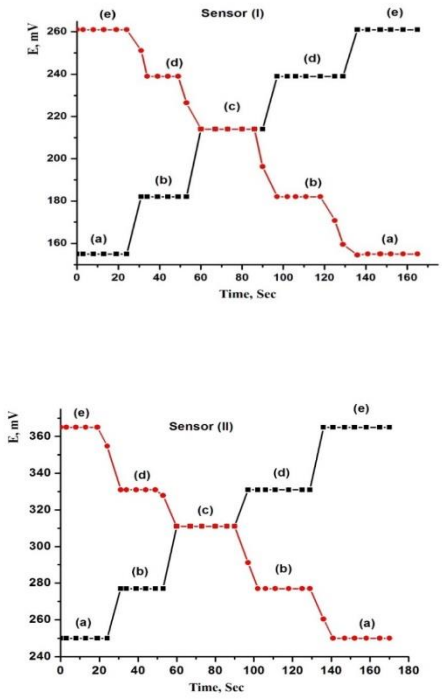

Figure 7: Dynamic response of the proposed Zn(II)-sensor (I and II) for step changes in Zn(II) concentration (from low to high and vice versa): (a) 1.0×10^{-6} mol L^{-1}, (b) 1.0×10^{-5} mol L^{-1}, (c) 1.0×10^{-4} mol L^{-1}, (d) 1.0×10^{-3} mol L^{-1} and (e) 1.0×10^{-2} mol L^{-1}

3.6. Effect of partially non-aqueous media on the prepared sensor response

The selective sensors must be able to function well in partly non-aqueous mediums since actual samples, particularly industrial effluents, may contain non-aqueous substances for the dissolution of chemicals [43]. Thus, it's important to look at how well the sensors work in mixed (water/organic) mixtures. The performance of the proposed mercury sensor (No. II) was tested in various ethanol-water and acetone-water combinations (v/v) mixes, however [43]. Table 1 presents the data. The working concentration range and Nernstian slope of the sensor were found to be lowered over the 25% non-aqueous content threshold. It was noted that the sensor functions adequately in mixes with up to 25% (v/v) non-aqueous medium content. Because of this, the sensor assembly may only be employed in non-aqueous media if the organic solvent level is less than 25% (Table 1) [43].

Table 1: Performance of the suggested Zn(II) (Sensor II) in partially non-aqueous media

Solvent	Volume of solvent (% v/v)	Working concentration range (mol L^{-1})	Slope (mV decade $^{-1}$)
Ethanol	10	1.0×10^{-7} to 1.0×10^{-2}	29.19
	15	1.0×10^{-7} to 1.0×10^{-2}	29.23
	20	1.0×10^{-7} to 1.0×10^{-2}	29.26
	25	5.0×10^{-7} to 1.0×10^{-2}	28.06
Acetone	10	1.0×10^{-7} to 1.0×10^{-2}	29.17
	15	1.0×10^{-7} to 1.0×10^{-2}	29.20
	20	1.0×10^{-7} to 1.0×10^{-2}	29.22
	25	5.0×10^{-7} to 1.0×10^{-2}	27.76

3.7. Lifetime and long-term stability of the proposed sensors

The repeatability and longevity of the sensors were checked by periodically examining the response of Zn(II) carbon paste (Sensors I and II) (Figure 8). The slope of the sensors was found to be 28.43±0.63 and 29.27±0.48 mV $decade^{-1}$ for electrodes I and II, respectively, and detection limit is seen to have grown by a tiny factor during the extended periods of 97 and 115 days. Yet, the electrode properties drastically departed from the Nernstian behavior after four months. This may be explained by a reduction in the amount of plasticizer and ionophore in the paste as a result of their migration. Consequently, the slope value, working concentration range, and detection limit of Zn(II)-MCPEs may be used for two to four months without any discernible change.

3.8. Effect of pH

The electrodes (I and II) were tested for their pH sensitivity in the pH range of 1.0- 10.0 at 1.0×10^{-3} and 1.0×10^{-5} mol L^{-1} Zn(II) ions concentrations. With the use of sodium hydroxide and diluted nitric acid solutions, the pH was corrected. Figure (9) illustrated the findings from the determination of the sensors' potential as a function of pH. As no interference from H^+ or OH^- was seen in the pH range of 3.5 - 8.0 and

3.0-8.5 for electrodes (I and II), respectively, it may be assumed that this pH range represents the functioning pH range of the sensors assembly. The interference of H+ ions increased at pH levels below 3.0 and reduces Zn(II) ion selectivity due to the quick rate of H^+ ion diffusion from sample solution to membrane matrix (extract H^+ ion), where they interact with carrier and undergo protonation. The sensors then react to hydrogen ions in this scenario. When the pH is greater than 8.5, some hydroxyl complexes of the Zn(II) ion develop in solution, which causes a divergence in the electrode response.

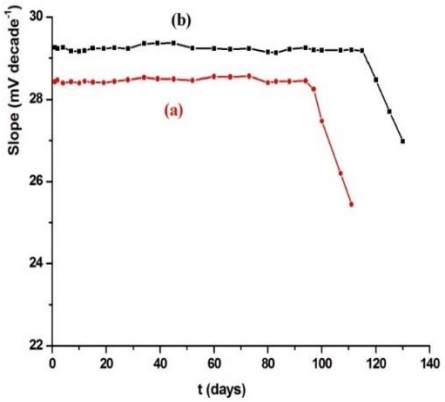

Figure 8: Effect of Lifetime on the performance characteristics of MCPE of (a) Sensor (I) and (b) Sensor (II).

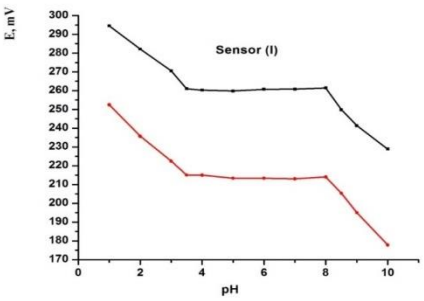

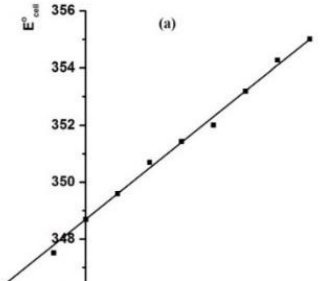

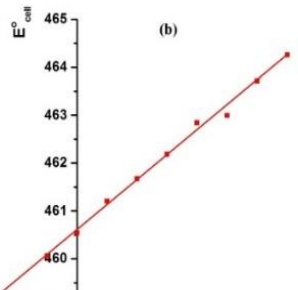

Figure 9: Effect of pH on the performance characteristics of MCPEs of Sensor (I) and Sensor (II).

3.9. Effect of temperature

At various temperatures, calibration graphs (E_{elec} vs p[Zn(II)]) were created on the test solution (10-60 °C) for the purpose of determining the isothermal coefficient (dE/dt) of the electrodes. In the temperature range, the electrodes behave in a Nernstian manner well. E^o_{cell} at various temperatures was obtained from calibration graphs as the intercepts at p[Zn(II)] = 0 and was plotted versus (t-25), where t was the temperature of the test solution in °C. After subtracting the values of the standard electrode potential of the Ag/AgCl electrode at these temperatures, t was the temperature of the test solution in °C. According to Andropov's equation, a straight-line plot is produced.

$$E^{\circ}_{Cell} = E^{\circ}_{Cell\,(25)} + (dE^{\circ}/dt)_{Cell}\,(t\text{-}25)$$

When T is the temperature in degrees Celsius, $E_{(25)}$ is the standard electrode potential at 25 °C, and the slope of the resulting straight line reflects the electrodes' isothermal coefficient. The isothermal coefficient for electrodes (I) and (II) was determined to be 0.000182 and 0.000104 mV/°C, respectively (Figure 10). The computed isothermal coefficient values for the electrodes show that electrode (II) has higher thermal stability than electrode (I) within the examined temperature range. With no discernible change in the sensors' (I) and (II) Nernstian behavior, the studied electrodes were determined to be useable up to 60 °C.

Figure 10: Effect of temperature on the performance characteristics of MCPEs of (a) Sensor (I) and (b) Sensor (II).

3.10. Potentiometric selectivity

Selectivity, which determines whether it is feasible to obtain an accurate measurement of the target ion in the presence of interfering species, is one of the most important properties of ion-selective sensors. Both the fixed interference technique (FIM) and the separate solution method (SSM) have been used to evaluate the recommended electrode's selectivity coefficient. Whereas the Nicolskii coefficient is determined by comparing the potential of two solutions that solely contain a salt of the main and interfering ions, the selectivity coefficient in SSM is derived using the following equation:

$$Ln_{IJ}^{SSM} = \frac{Z_I F \left[E_2 - E_1 \right]}{R T} - Ln\, a_I \left(1 - \frac{Z_I}{Z_J} \right)$$

In this equation, it is assumed that $a_I = a_J$. The electrode's responses to the principal and interfering ions are represented by the letters E_1 and E_2, respectively. The selectivity coefficient in the FIM, on the other hand, was calculated using potential measurements on solutions with varying quantities of Zn(II) ions and a constant concentration of interfering ion (1.0×10^{-3} mol L^{-1}). The following equation is used to compute the selectivity coefficient:

$$K_{I,J}^{FIM} = \frac{a_I(DL)}{(a_J^{Z_I/Z_J}}$$

Where a_I (DL) is the primary ion activity at the limit of detection, a_J is the activity of the interference ion (1.0×10^{-3} mol L^{-1}), Z_I and Z_J are the primary charge and the charge of interference ions, respectively. It can be seen from Table 2, that the proposed electrode is highly selective with regards to a range of cations towards Zn(II) ions. The two sets of results acquired using the SSM and FIM approaches are in satisfactory agreement. The fact that the computed selectivity coefficient values are less than 1 and that foreign ions have little to no effect on the performance of Zn(II) ion-selective electrodes is clearly demonstrated by this. Table provides a list of all of these outcomes in tabular format (2).

Table 2: Selectivity coefficients of various ions using MCPE (Sensor I and II).

Interfering ions	$-\log K^{SSM}_{I,J}$ Sensor (I)	$-\log K^{SSM}_{I,J}$ Sensor (II)	$-\log K^{FIM}_{I,J}$ Sensor (I)	$-\log K^{FIM}_{I,J}$ Sensor (II)
Ca^{2+}	4.67	4.78	4.35	5.23
Cd^{2+}	4.53	4.69	4.26	4.92
Cu^{2+}	4.12	4.32	4.01	4.61
Ba^{2+}	5.01	5.21	4.95	5.64
Mg^{2+}	5.56	5.73	4.99	5.93
Hg^{2+}	3.15	3.62	3.04	3.77
Al^{3+}	4.96	4.99	4.89	5.29
Fe^{3+}	2.42	2.63	2.21	2.71
Ce^{3+}	3.01	3.27	2.89	3.34
Bi^{3+}	5.76	5.93	5.15	6.29
Na^{+}	5.99	6.05	5.67	6.72
K^{+}	5.51	5.68	5.37	5.87
Sr^{2+}	4.01	4.32	4.17	4.63
Mn^{2+}	4.84	4.98	4.63	4.88
Pb^{2+}	5.03	5.63	5.34	5.71
Co^{2+}	3.97	4.24	4.17	4.42
Ni^{2+}	4.45	4.74	4.56	4.82
I^{-}	4.53	4.73	4.07	4.81
Cl^{-}	5.71	5.92	5.49	6.17
Br^{-}	5.47	5.61	5.21	5.84
CN^{-}	5.77	5.96	5.56	6.41
CO_3^{2-}	4.89	4.93	4.42	5.27
SO_4^{2-}	5.18	5.32	5.09	5.77

3.11. Proposed sensor reproducibility

These sensors (I and II) were produced using the best paste composition to verify their repeatability, and their responses to Zn(II) ion concentration were measured. The outcomes demonstrated that the average slopes, detection limits, and linear dynamic ranges were 28.43±0.63 mV decade^{-1}, 29.72±0.48 mV decade^{-1}, 1x10^{-7} mol L^{-1}, and 1x10^{-7} – 1x10^{-1} mol L^{-1}, respectively (Table 3).

Table 3. Response characteristics of MCPEs (Sensors I and II).

Items	Sensor (I)	Sensor (II)
Slope (mV decade^{-1})	28.43±0.63	29.27±0.48
Usable range (mol L^{-}	1.0 ×10^{-7} – 1.0 ×10^{-1}	1.0 × 10^{-7}- 1.0 × 10^{-1}
Lower detection limit	1.0 × 10^{-7}	1.0 × 10^{-7}
Intercept (mV)	351.97 ±2.04	454.15 ± 1.83
Working pH range	3.5 - 8.0	3.0 - 8.5
Lifetime (days)	97	115
Response time (s)	7	5
Correlation	0.989	0.998
Accuracy (%)	98.27	99.19
Precision (%)	0.79	0.36

3.12. Analytical applications

The analytical usefulness of the suggested sensors system has been shown through the detection

of Zn(II) ions in diverse water samples. In a 100 mL volumetric flask, the resultant solution was diluted with distilled water. Acetate buffer solution was used to raise the pH of the water sample to 4.0 after adding Zn(II) solution at various concentrations. The calibration plot approach was used to directly quantify the Zn(II) content in the real water samples that had been spiked. Atomic absorption spectroscopy was also used to determine the outcomes (AAS). Upon comparing the findings of each water sample's analysis to those obtained by AAS, it was clear that the determination of Zn(II) ion was accurate enough (Table 4). As a result, the sensors offered an excellent alternative for finding Zn(II) in various genuine samples.

Table 4: Determination of Zn(II) ions in spiked petroleum wells water samples using MCPE (Sensor I and Sensor II).

Samples	[Zn(II)] (mg L^{-1})									
	Sensor (I)				Sensor (II)			AAS		
	Added	Found	R.S.D (%)	Recovery (%)	Found	R.S.D (%)	Recovery (%)	Found	R.S.D (%)	Recovery (%)
1	0.65	0.62	1.241	95.38	0.64	0.825	98.46	0.6	2.617	93.84
	1.0	0.96	1.107	96.0	0.98	0.913	98.0	0.9	2.281	95.0
2	0.60	0.57	2.046	95.0	0.59	0.458	98.33	0.5	2.782	91.67
	0.85	0.83	1.836	97.65	0.84	0.317	98.82	0.8	2.419	95.29
3	0.95	0.91	1.759	95.79	0.93	0.142	97.89	0.8	2.945	93.68
	1.25	1.20	1.519	96.0	1.22	0.209	97.60	1.1	2.884	94.40
4	1.0	0.98	0.638	98.00	0.99	0.261	99.0	0.9	1.026	96.00
	1.55	1.51	0.669	97.41	1.53	0.293	98.71	1.4	0.980	96.13

3.13. Comparison study

The data in (Table 5) compare the detection limit, linear range, response time, pH and slope of the suggested electrodes with many pastly published Zn(II)-selective electrodes. It is noteworthy that the suggested electrodes have much superior selectivity coefficients, linear range, slope, and response times than the previously reported Zn(II)-selective electrodes [13, 44-50]. (Table 5).

Table 5. Comparing some of the Zn(II)-MCPE (Sensors I and II) characteristics with some of the previously reported Zn(II)-ISEs.

References	Slope (mV $decade^{-1}$)	Respons time (s)	pH	Lifetime (months)	Linear range (mol L^{-1})	DL (mol L^{-1})
Sensor	28.43	7	3.5 – 8.0	<3	$1.0 \times 10^{-7} – 1.0 \times 10^{-1}$	1.0×10^{-7}
Sensor	29.27	5	3.0 - 8.5	>4	$1.0 \times 10^{-7} – 1.0 \times 10^{-1}$	1.0×10^{-7}
13	30.0	<5	5.0–10.0	-	$1.0 \times 10^{-1} – 1.0 \times 10^{-5}$	6.50×10^{-6}
44	28.0	5	4.0–11.0	-	$1.0 \times 10^{-5} – 1.0 \times 10^{-1}$	1.17×10^{-6}
45	27.12	5	4.4-8.0	5	$1.0 \times 10^{-5} – 1.0 \times 10^{-1}$	8.0×10^{-6}
46	29.80	6	3.0- 7.5	22	$2.62 \times 10^{-1} - 6.54 \times 10^{5}$	1.93×10^{-1}
47	29.69	20	2.7- 7.0	-	$1.0 \times 10^{-1} - 3.09 \times 10^{-7}$	1.9×10^{-7}
48	29.45	14	4 – 6	-	$2.5 \times 10^{-6} - 1.0 \times 10^{-1}$	1.0×10^{-6}
49	28.5	<10	2.5–8.5	-	$2.82 \times 10^{-6} - 1.0 \times 10^{-1}$	2.24×10^{-6}
50	26.5	10	3.0 – 6.0	8	$5.0 \times 10^{-5} - 1.0 \times 10^{-1}$	3.0×10^{-5}

4. Conclusion

Based on the molecular imprinting method, highly sensitive and selective electrochemical sensors were fabricated and used to quantify Zn(II) ion in spiked petroleum water samples. Comparing the suggested sensors to previous Zn(II) detection techniques, it demonstrated strong sensitivity, high repeatability, and great stability. The proposed potentiometric sensor's response characteristics were compared to those of potentiometric sensors previously disclosed, and the outcomes showed that the presented sensors consistently outperformed the latter in terms of detection limits and, more importantly, selectivity over other metal ions. It may be used to assess Zn(II) levels in various water samples. This technique worked effectively to evaluate Zn(II) ions in a variety of genuine samples, and the results were in good agreement with those obtained from AAS.

References

[1] H. Wu, G. Lin, C. Liu, S. Chu, C. Mo, X. Liu, Progress and challenges in molecularly imprinted polymers for adsorption of heavy metal ions from wastewater, Trends in Environmental Analytical Chemistry, 36 (2022) e00178.

[2] S. Rahman, B. Bozal-Palabiyik, D.N. Unal, C. Erkmen, M. Siddiq, A. Shah, B. Uslu, Molecularly imprinted polymers (MIPs) combined with nanomaterials as electrochemical sensing applications for environmental pollutants, Trends in Environmental Analytical Chemistry, 36 (2022) e00176.

[3] C.C. Eylem, M. Taştekin, A. Kenar, Simultaneous determination of copper and zinc in brass samples by PCR and PLS1 methods using a multiple ion-selective electrode array, Talanta, 183 (2018) 184-191.

[4] A.V. Blinov, S.A. Siddiqui, A.A. Nagdalian, A.A. Blinova, A.A. Gvozdenko, V.V. Raffa, N.P. Oboturova, A.B. Golik, D.G. Maglakelidze, S.A. Ibrahim, Investigation of the influence of Zinc-containing compounds on the components of the colloidal phase of milk, Arabian Journal of Chemistry, 14 (2021) 103229.

[5] G. López-Gálvez, M. López-Alonso, A. Pechova, B. Mayo, N. Dierick, J. Gropp, Alternatives to antibiotics and trace elements (copper and zinc) to improve gut health and zootechnical parameters in piglets: A review, Animal Feed Science and Technology, 271 (2021) 114727.

[6] A.A. Skalny, Y.S. Medvedeva, I.B. Alchinova, E.R. Gatiatulina, I.V. Radysh, M.Y. Karganov, A.V. Skalny, A.A. Nikonorov, A.A. Tinkov, Zinc supplementation modifies trace element status in exercised rats, Journal of Applied Biomedicine, 15 (2017) 39-47.

[7] B.P.S. Gautam, M. Gondwal, R.R. Maurya, P. Singh, R.L. Prasad, I. Bahadur, Synthesis, spectroscopic, solid-state electrical conductivity, and thermal analysis of Cu(II) doped Zn(II) heterobimetallic complexes derived from 2,5-dichloro-3,6-bis-(methylamino)1,4-benzoquinone, Colloids and Surfaces A: Physicochemical and Engineering Aspects, 647 (2022) 129071.

[8] A.A. Khandar, Z. Mirzaei-Kalar, J. White, S.A. Hosseini-Yazdi, A. Jouyban, Synthesis, X-ray crystal structure and solubility of a new zinc–naproxen complex: Potentiometric and thermodynamic studies in methanol + water mixtures, Journal of Molecular Liquids, 224 (2016) 684-693.

[9] A.A. Khandar, Z. Mirzaei-Kalar, J.M. White, S.A. Hosseini-Yazdi, A. Kebriaeezadeh, A. Jouyban, Solubility, potentiometric and thermodynamic studies on zinc-bosentan complex; synthesis and X-ray crystal structure, Journal of Molecular Liquids, 234 (2017) 64-72.

[10] M.B. Zobkov, M.V. Zobkova, New spectroscopic method for true color determination in natural water with high agreement with visual methods, Water Research, 177 (2020) 115773.

[11] S.-F. Huang, W.-L. Shih, Y.-Y. Chen, Y.-M. Wu, L.-C. Chen, Ion composition profiling and pattern recognition of vegetable sap using a solid-contact ion-selective electrode array, Biosensors and Bioelectronics: X, 9 (2021) 100088.

[12] A.S. Amin, S. El-Bahy, H.H. El-Feky, Utility of 5-(2′,4′-dimethylphenylazo)-6-hydroxy-pyrimidine-2,4-dione in PVC membrane for a novel green optical chemical sensor to detect zinc ion in environmental samples, Analytical Biochemistry, 643 (2022) 114579.

[13] Ö. Isildak, F.B. Egeli, O. Özbek, The use of different ionophores for the determination of

Zn2+ ions, Sensors International, 3 (2022) 100195.

[14] X. Wu, Y. Zhu, S. Bao, J. Cao, C. Zhao, X. Zhao, Z. Liu, X. Wang, Y. Fu, A novel and specific molecular imprinted polymer using cellulose as a carrier for the targeted separation of quercetin from Sophora Japonica, Materials Today Communications, 32 (2022) 104168.

[15] J. Pan, S. Liu, H. Jia, J. Yang, M. Qin, T. Zhou, Z. Chen, X. Jia, T. Guo, Rapid hydrolysis of nerve agent simulants by molecularly imprinted porous crosslinked polymer incorporating mononuclear zinc(II)-picolinamine-amidoxime module, Journal of Catalysis, 380 (2019) 83-90.

[16] A. Kliangsuwan, A. Phonchai, O. Bunkoed, A magnetic molecularly imprinted polymer hierarchical composite adsorbent embedded with a zinc oxide carbon foam nanocomposite for the extraction of sulfonamides, Microchemical Journal, 179 (2022) 107443.

[17] J. Tang, Y. Ren, L. Zhu, Y. Chen, S. Liu, L. Zhu, R. Yang, Magnetic molecularly imprinted polymer combined with solid-phase extraction for detection of kojic acid in cosmetic products, Microchemical Journal, 183 (2022) 108028.

[18] D.-H.-N. Nguyen, Q.-H. Le, T.-L. Nguyen, V.-T. Dinh, H.-N. Nguyen, H.-N. Pham, T.-A. Nguyen, L.-L. Nguyen, T.-M.-T. Dinh, V.-Q. Nguyen, Electrosynthesized nanostructured molecularly imprinted polymer for detecting diclofenac molecule, Journal of Electroanalytical Chemistry, 921 (2022) 116709.

[19] J. Pu, H. Wang, C. Huang, C. Bo, B. Gong, J. Ou, Progress of molecular imprinting technique for enantioseparation of chiral drugs in recent ten years, Journal of Chromatography A, 1668 (2022) 462914.

[20] Q. Li, T. Wang, Y. Jin, C. Wierzbicka, F. Wang, J. Li, B. Sellergren, Synthesis of highly selective molecularly imprinted nanoparticles by a solid-phase imprinting strategy for fluorescence turn-on recognition of phospholipid, Sensors and Actuators B: Chemical, 368 (2022) 132193.

[21] M. Harijan, V. Shukla, A.K. Singh, R. Raghuwanshi, G. Nath, M. Singh, Design of molecularly imprinted sensor for detection of typhoid using immunoinformatics and molecular imprinting, Biosensors and Bioelectronics: X, 10 (2022) 100090.

[22] K. Prabakaran, P.J. Jandas, J. Luo, C. Fu, A highly sensitive surface acoustic wave sensor modified with molecularly imprinted hydrophilic PVDF for the selective amino acid detection, Sensors and Actuators A: Physical, 341 (2022) 113525.

[23] M. Ardalani, M. Shamsipur, A. Besharati-Seidani, A new generation of highly sensitive potentiometric sensors based on ion imprinted polymeric nanoparticles/multiwall carbon nanotubes/polyaniline/graphite electrode for sub-nanomolar detection of lead(II) ions, Journal of Electroanalytical Chemistry, 879 (2020) 114788.

[24] J. Wang, R. Liang, W. Qin, Molecularly imprinted polymer-based potentiometric sensors, TrAC Trends in Analytical Chemistry, 130 (2020) 115980.

[25] M. Wadie, H.M. Marzouk, M.R. Rezk, E.M. Abdel-Moety, M.A. Tantawy, A sensing platform of molecular imprinted polymer-based polyaniline/carbon paste electrodes for simultaneous potentiometric determination of alfuzosin and solifenacin in binary co-formulation and spiked plasma, Analytica Chimica Acta, 1200 (2022) 339599.

[26] T. Alizadeh, K. Atayi, Synthesis of hydrogen phosphate anion-imprinted polymer via emulsion polymerization and its use as the recognition element of graphene/graphite paste potentiometric electrode, Materials Chemistry and Physics, 209 (2018) 180-187.

[27] M.A. Hammam, H.A. Wagdy, R.M. El Nashar, Moxifloxacin hydrochloride electrochemical detection based on newly designed molecularly imprinted polymer, Sensors and Actuators B: Chemical, 275 (2018) 127-136.

[28] T. Alizadeh, S. Nayeri, S. Mirzaee, A high performance potentiometric sensor for lactic acid determination based on molecularly imprinted polymer/MWCNTs/PVC nanocomposite film covered carbon rod electrode, Talanta, 192 (2019) 103-111.

[29] K. Liu, Y. Song, D. Song, R. Liang, Plasticizer-free polymer membrane potentiometric sensors based on molecularly imprinted polymers for determination of neutral phenols, Analytica Chimica Acta, 1121 (2020) 50-56.

[30] Widayani, Yanti, T.D.K. Wungu, Suprijadi, Preliminary Study of Molecularly Imprinted

Polymer-based Potentiometric Sensor for Glucose, Procedia Engineering, 170 (2017) 84-87.

[31] T.S. Anirudhan, S. Alexander, A potentiometric sensor for the trace level determination of hemoglobin in real samples using multiwalled carbon nanotube based molecular imprinted polymer, European Polymer Journal, 97 (2017) 84-93.

[32] S.A. Rezvani Ivari, A. Darroudi, M.H. Arbab Zavar, G. Zohuri, N. Ashraf, Ion imprinted polymer based potentiometric sensor for the trace determination of Cadmium (II) ions, Arabian Journal of Chemistry, 10 (2017) S864-S869.

[33] M.F. Abdel-Ghany, L.A. Hussein, N.F. El Azab, Novel potentiometric sensors for the determination of the dinotefuran insecticide residue levels in cucumber and soil samples, Talanta, 164 (2017) 518-528.

[34] T.G. Costa, L. Meurer, G.A. Micke, S. Gonçalves, B. Szpoganicz, A.S. Mangrich, Potentiometric titration of microhydrolysis products of oils: A new low-cost methodology and investment for the analysis of oil binders present in works of art, Talanta, 212 (2020) 120736.

[35] P. Phansi, S.L.C. Ferreira, V. Cerdà, Accurate calculation of equilibrium constants using potentiometric titrations, TrAC Trends in Analytical Chemistry, 155 (2022) 116676.

[36] S. Kounbach, M. Ben Embarek, L. Mahi, R. Boulif, R. Beniazza, R. Benhida, Simultaneous determination of H2SiF6, HF and total fluoride in fluorosilicic acid recovered from wet phosphoric acid production by potentiometric titration, Microchemical Journal, 175 (2022) 107152.

[37] M. Saber-Tehrani, M. Vardini, P. Aberoomand azar, S. Husain, Molecularly Imprinted Polymer Based PVC-Membrane-Coated Graphite Electrode for the Determination of Metoprolol, Int. J. Electrochem. Sci. International Journal, 5 (2010) 88-104.

[38] B.P. Branchaud, Molecularly Imprinted Materials: Science and Technology Edited by Mingdi Yan (Portland State University) and Olof Ramström (Royal Institute of Technology, Stockholm). Marcel Dekker: New York. 2005. xiv + 734 pp. $179.95. ISBN 0-8247-5353-4, Journal of the American Chemical Society, 127 (2005) 14117-14118.

[39] K. Subashini, S. Prakash, V. Sujatha, Biological applications of green synthesized zinc oxide and nickel oxide nanoparticles mediated poly(glutaric acid-co-ethylene glycol-co-acrylic acid) polymer nanocomposites, Inorganic Chemistry Communications, 139 (2022) 109314.

[40] M. Medimagh, N. Issaoui, S. Gatfaoui, S. Antonia Brandán, O. Al-Dossary, H. Marouani, M. J. Wojcik, Impact of non-covalent interactions on FT-IR spectrum and properties of 4-methylbenzylammonium nitrate. A DFT and molecular docking study, Heliyon, 7 (2021) e08204.

[41] V.A. Minaeva, N.N. Karaush-Karmazin, A.A. Panchenko, D.N. Heleveria, B.F. Minaev, Hirshfeld surfaces analysis and DFT study of the structure and IR spectrum of N-ethyl-2-amino-1-(4-chlorophenyl)propan-1-one (4-CEC) hydrochloride, Computational and Theoretical Chemistry, 1205 (2021) 113455.

[42] M. Wadie, E.M. Abdel-Moety, M.R. Rezk, A.M. Mahmoud, H.M. Marzouk, Electro-polymerized poly-methyldopa as a novel synthetic mussel-inspired molecularly imprinted polymeric sensor for darifenacin: Computational and experimental study, Applied Materials Today, 29 (2022) 101595.

[43] A. Shirzadmehr, A. Afkhami, T. Madrakian, A new nano-composite potentiometric sensor containing an Hg2+-ion imprinted polymer for the trace determination of mercury ions in different matrices, Journal of Molecular Liquids, 204 (2015) 227-235.

[44] Ö. Isildak, O. Özbek, K.M. Yigit, Zinc(II)-selective PVC membrane potentiometric sensor for analysis of Zn2+ in drug sample and different environmental samples, International Journal of Environmental Analytical Chemistry, 101 (2021) 2035-2045.

[45] A. Sharifi, L. Hajiaghababaei, S. Suzangarzadeh, M.R.J. Sarvestani, Synthesis of 3-((6-methyl-5-oxo-3-thioxo-2,5-dihydro-1,2,4-triazin-4(3H)-yl)imino)indolin-2-one as an excellent ionophore to the construction of a potentiometric membrane sensor for rapid determination of

zinc, Analytical and Bioanalytical Electrochemistry, 9 (2017) 888-903.

[46] A. Shirzadmehr, M. Rezaei, H. Bagheri, H. Khoshsafar, Novel potentiometric sensor for the trace-level determination of Zn2+ based on a new nanographene/ion imprinted polymer composite, International Journal of Environmental Analytical Chemistry, 96 (2016) 929-944.

[47] R. Isaac, P. Prabhakaran, Artificial neural network optimization of a carbon paste electrode for the detection of zinc ions, Nano Biomedicine and Engineering, 8 (2016) 47-53.

[48] A.A. Bazrafshan, S. Hajati, M. Ghaedi, Improvement in the performance of a zinc ion-selective potentiometric sensor using modified core/shell Fe3O4@SiO2 nanoparticles, RSC Advances, 5 (2015) 105925-105933.

[49] A.K. Singh, A.K. Jain, P. Saxena, S. Mehtab, Zn(II)-selective membrane electrode based on tetraazamacrocycle [Bzo 2Me2Ph2(16)hexaeneN4], Electroanalysis, 18 (2006) 1186-1192.

[50] A.R. Fakhari, M. Shamsipur, K. Ghanbari, Zn(II)-selective membrane electrode based on tetra(2-aminophenyl) porphyrin, Analytica Chimica Acta, 460 (2002) 177-183.